Theory of the π State in ^{3}He Josephson Junctions

J. K. Viljas and E. V. Thuneberg

Low Temperature Laboratory, Helsinki University of Technology, FIN-02015 HUT, Finland

(Received 13 July 1999)

The flow of superfluid ^{3}He-B through a 65×65 array of nanometer-size apertures has been measured recently by Backhaus *et al.* They find in the current-phase relation a new branch, the so-called π state. We study two limiting cases which show that the π state arises from the coupling of the phase degree of freedom to the spin-orbit rotation. The π state exists in a single large aperture, but is difficult to observe because of hysteresis. A better correspondence with experiments is obtained by assuming a thin wall, where the Josephson coupling between the two sides arises from a dense array of pinholes.

PACS numbers: 67.57.Np

The flow of superfluid ^{3}He-B through a single nanometer-size aperture was studied by Avenel and Varoquaux some time ago [1]. At temperatures near the superfluid transition temperature T_c, the current-phase relation is sinusoidal

$$J(\phi) = J_c \sin\phi \,, \tag{1}$$

as expected for a Josephson junction. Also according to expectation, they find that the sine form (1) gradually becomes tilted when the temperature is lowered. More recently, Backhaus *et al.* studied a 65×65 array of small apertures [2,3]. They discovered a new behavior, where the current-phase relation acquires a positive slope at phase differences $\phi \approx \pi$. This π state develops when the temperature is lowered to approximately $0.6T_c$.

A few theoretical explanations for the π state have been proposed [4,5]. In this Letter we present a theory that is based on the many-component form of the order parameter in ^{3}He. It differs from the previous suggestions because it contains no unjustified assumptions, and an order-of-magnitude agreement with experiments is obtained without any adjustable parameters.

Unusual current-phase relations also occur in other systems. A π junction, where J_c in (1) is negative, can be induced by adding magnetic impurities to a tunneling barrier between two s-wave superconductors [6]. Similar π shifts appear in nonmagnetic junctions between d-wave superconductors. In addition, current-phase relations with additional zeros [$J(\phi) = 0$ for $\phi \neq 0$ or π] can appear for special orientations of the anisotropic crystals [7]. The π state in ^{3}He differs from these in several respects, most fundamentally because it arises from the interplay of two soft modes of the order parameter, the phase ϕ and the spin-orbit rotation.

We present calculations in two limiting cases. In the case of a tunneling barrier, the existence of the π state can be demonstrated by analytic calculations. The parameters of the tunneling model are estimated using the quasiclassical theory. In the case of a single aperture, the π state is obtained by numerical simulations using the Ginzburg-Landau theory of ^{3}He.

Tunneling junction.—The simplest case to demonstrate the π state is to consider a planar wall through which the ^{3}He atoms can tunnel. The energy arising from tunneling between the left (L) and right (R) sides can be written as [8]

$$F_J = -\mathrm{Re}\sum_\mu [a A^{L*}_{\mu z} A^R_{\mu z} + b(A^{L*}_{\mu x} A^R_{\mu x} + A^{L*}_{\mu y} A^R_{\mu y})] . \tag{2}$$

Here $A_{\mu j}$ is the 3×3 matrix order parameter, where the first index μ refers to the orientation of the Cooper pair in spin space and the latter index j in orbital space. The z axis is taken perpendicular to the tunneling wall. Equation (2) is a simple generalization of $F_J = -a\,\mathrm{Re}(A^{L*}A^R)$, which describes the Josephson coupling of two s-wave superconductors with order parameters A^L and A^R [9]. The mass current through the wall is given by $J = (2m_3/\hbar)\partial F_J/\partial\phi$, where $\phi = \phi^L - \phi^R$ is the phase difference and m_3 is the mass of a ^{3}He atom.

In the B phase of ^{3}He, the order parameter has the form $A_{\mu j} = \Delta \exp(i\phi) R_{\mu j}$. Here Δ is the amplitude, $\exp(i\phi)$ is a phase factor, and $R_{\mu j}$ is a 3×3 rotation matrix: $\sum_\mu R_{\mu j} R_{\mu k} = \delta_{jk}$. The rotation matrices can be parametrized by an axis $\hat{\mathbf{n}}$ and an angle θ. Substituting into (2) gives (α, $\beta > 0$),

$$F_J = -\sum_\mu [\alpha R^L_{\mu z} R^R_{\mu z} + \beta(R^L_{\mu x} R^R_{\mu x} + R^L_{\mu y} R^R_{\mu y})] \cos\phi \,. \tag{3}$$

In deriving this expression from (2), one must pay attention to the fact that the order parameter of the p-wave superfluid is strongly suppressed near a wall. As a consequence the parameters α and β in (3) are not simply related to the coefficients a and b in (2), but otherwise the dependence of F_J on the soft variables ϕ and $R_{\mu j}$ remains the same as obtained by the simple substitution above.

Let us consider the case that the rotation matrices on the left and right sides are the same. This gives rise to the "zero state" with the critical current $J_c = (2m_3/\hbar)(\alpha + 2\beta) > 0$. This state has the lowest energy when $|\phi| < \pi/2$ because it corresponds to the maximum of the expression in square brackets in (3). The situation changes when ϕ exceeds $\pi/2$. There, one has to look for a *minimum* of the expression in the square brackets. This corresponds to the π state, which is illustrated by the solid

line in Fig. 1a. The critical current J_c in (1) is negative: $J_c = -(2m_3/\hbar)\alpha$ if $\alpha > \beta$ and $J_c = -(2m_3/\hbar)(2\beta - \alpha)$ otherwise.

In order to make the tunneling model realistic, we have to consider three additional contributions to the energy. Firstly, there is the magnetic dipole-dipole energy $F_d = 8g_d\Delta^2(\frac{1}{4} + \cos\theta)^2$ [10]. In the bulk it fixes the rotation angle θ equal to $\theta_0 = \arccos(-\frac{1}{4}) = 104°$. This also remains valid near the junction because both the Josephson energy (3) and the dipole-dipole energy can reach their minima simultaneously: the products of two rotation matrices appearing in the former are not limited by the fact that both matrices have a fixed rotation angle θ_0. Secondly, there is a surface energy that arises from the coupling of the dipole-dipole energy to the suppression of the order parameter near walls [11]. It has the form

$$F_s = b_4(\hat{\mathbf{n}} \cdot \hat{\mathbf{s}})^4 - b_2(\hat{\mathbf{n}} \cdot \hat{\mathbf{s}})^2, \quad (4)$$

where $\hat{\mathbf{s}}$ is the surface normal. The lowest surface energy is achieved when the rotation axis $\hat{\mathbf{n}}$ is perpendicular to the wall, $\hat{\mathbf{n}} = \pm\hat{\mathbf{s}}$, because $b_2 > 2b_4 > 0$. Thirdly, there is a gradient energy associated with the spatial bending of the rotation axis $\hat{\mathbf{n}}$. It arises because in practice all tunnel junctions are of finite size, and other walls in the container favor a different orientation of $\hat{\mathbf{n}}$ than may be the minimum of the Josephson energy. We model the gradient energy by the simple quadratic forms

$$F_g^L = \gamma(\eta^L - \eta_\infty^L)^2, \qquad F_g^R = \gamma(\eta^R - \eta_\infty^R)^2, \quad (5)$$

where η is the polar angle of $\hat{\mathbf{n}}$, i.e., $\cos\eta = \hat{n}_z$. η^L and η^R denote the polar angles on both sides just at the junction, and we assume that the values η_∞^L and η_∞^R farther away are either 0 or π. In the experimental case [2] the surface energy (4) is important in fixing η_∞^L and η_∞^R, but otherwise its contribution is so small that we can neglect it in the following.

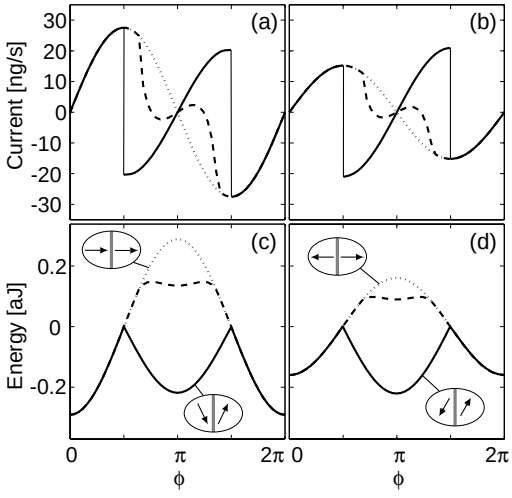

FIG. 1. The current-phase relationships and energies for the tunneling model. The left and right panels correspond to parallel and antiparallel $\hat{\mathbf{n}}$'s far away from the junction, respectively. The directions near the junction are depicted by arrows. The curves correspond to different values of the gradient-energy parameter γ: ideal π state ($\gamma = 0$, solid line), no π state ($\gamma = \infty$, dotted line), and an intermediate case ($\gamma = 0.245$ aJ, dashed line). The parameters $\alpha = 0.2207$ aJ and $\beta = 0.0347$ aJ (1 aJ $= 1 \times 10^{-18}$ J) are chosen to imitate the experiment [3] at $T = 0.55T_c$.

The current-phase relations for the tunneling model, (3) and (5), are plotted in Fig. 1. It can be seen that a large value of the gradient energy parameter γ suppresses the π state. Furthermore, we find two cases where the rotation axes $\hat{\mathbf{n}}$ far from the junction are either parallel or antiparallel. The latter has a smaller critical current [$J_c = (2m_3/\hbar)(\alpha - \frac{7}{4}\beta)$] but a relatively more pronounced π state. This "bistability" was theoretically discussed in Ref. [12] and has recently been observed experimentally [3].

Evaluation of tunneling parameters.—The experiment [2] has a square array of apertures of diameter $D = 100$ nm with spacing $S = 3$ μm in a wall of thickness $W = 50$ nm. In order to make the tunneling model imitate the experiment, we estimate α and β by letting all three lengths approach zero but keeping their ratios unchanged [13]. The calculation for such "pinholes" [14] is relatively simple once the self-consistent solution for the order parameter near a wall is known [15]. We assume diffuse scattering of quasiparticles at surfaces. The tunneling form (3) is reproduced in these calculations at temperatures $T \gtrsim 0.5T_c$, and values of α and β can be extracted. The parameter γ can be estimated using the bending energy of the B phase [16] and assuming a simple form $\eta(\mathbf{r}) - \eta_\infty \propto r^{-1}$, where r is the radius from the center of the aperture array, and this expression is cut off at the radius of the array. In agreement with experiments, we find that the π state appears at low temperatures because α and $\beta \propto (1 - T/T_c)^2$ have stronger temperature dependence than $\gamma \propto 1 - T/T_c$ (see Fig. 2). Moreover, the parameters α, β, and γ agree within 1 order of magnitude to those that give an approximate best fit to the experiments (see caption of Fig. 2). This fit reproduces also the absolute magnitude of

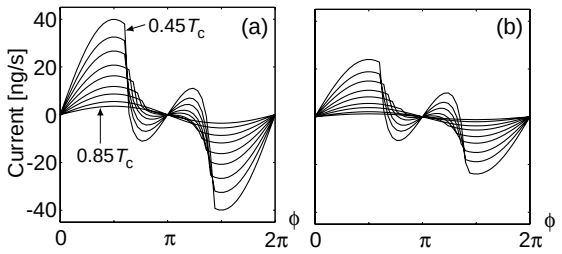

FIG. 2. The current-phase relationships for parallel (a) and antiparallel (b) $\hat{\mathbf{n}}$'s far away from the junction. The different curves correspond to temperatures from $0.45T_c$ to $0.85T_c$ with intervals of $0.05T_c$. The parameters α and β are calculated with the pinhole model and γ is estimated as explained in the text. However, in order to get better correspondence with experiments, we have multiplied the estimated values by factors 7.5, 1.3, and 0.15, respectively.

the critical current, and the same values of the parameters are used for cases of both parallel and antiparallel $\hat{\mathbf{n}}$'s.

The tunneling model can be improved trivially by extending the pinhole calculation to the whole temperature range $0 < T < T_c$. A more ambitious project for the future would be the self-consistent calculation for aperture sizes on the order of the coherence length ξ_0. In both cases the resulting Josephson energy $F_J(\phi, R^L_{\mu j}, R^R_{\mu j})$ will no longer be of the simple form (3).

Single aperture.—The limit opposite to the tunneling barrier is a single large aperture. There the major task is to calculate the order parameter self-consistently. We have done this using the Ginzburg-Landau (GL) theory of ^{3}He. The differential equations were solved numerically on a grid in and around the aperture. Our calculations are more general than the previous ones [12,17] because we use a full three-dimensional grid. Vanishing $A_{\mu j}$ was assumed at surfaces.

The order parameter of the π state is shown in Fig. 3. It is plotted along the axis of a circularly symmetric aperture. For simplicity, we have normalized the order parameter to a unit matrix in the bulk, $A_{\mu j}(z = \pm\infty) = \exp(\pm i\phi/2)\delta_{\mu j}$ (assuming the case of parallel $\hat{\mathbf{n}}$'s). This is possible because for aperture sizes on the order of the GL coherence length ξ_{GL}, the dipole-dipole energy can be neglected. The characteristic property of the π state is the components A_{yz} and A_{zy}. These are the dominant components in the orifice, and they decay slowly towards the bulk. They imply broken symmetry: the symmetry group of the π branch is $m'm2'$ compared to $\frac{\infty}{m'}\frac{2'}{m}$ of the zero branch. (Here prime denotes time-inversion.) This sets a rather strong requirement for the calculation because the circular symmetry of the aperture cannot be used to simplify the computation. The current-phase relations are summarized in Fig. 4.

We see that the occurrence of the π branch depends sensitively on the diameter of the aperture, whereas the wall thickness is less important. For small apertures no π branch is found. When D exceeds approximately $5\xi_{GL}$, the π branch appears. In the region (*b*) the current-phase relation has negative slope. Such a state can be stabilized if the left and right sides are connected, such as in a torus geometry. By increasing the diameter, the current-phase relation gets a positive slope in region (*c*). This state is stable also in a piston-driven flow channel. The π state is also the absolute energy minimum at $\phi = \pi$ in region (*c*). In region (*d*) the π state continues to exist but it has higher energy than the zero branch. The calculation assumes the idealized case of flow between two infinite bulk fluids. Any additional hydrodynamic inductance shifts upwards at the border between regions (*c*) and (*d*) as it increases the energy of current carrying states.

Although the π branch constitutes the absolute energy minimum, it may be difficult to find it experimentally in a

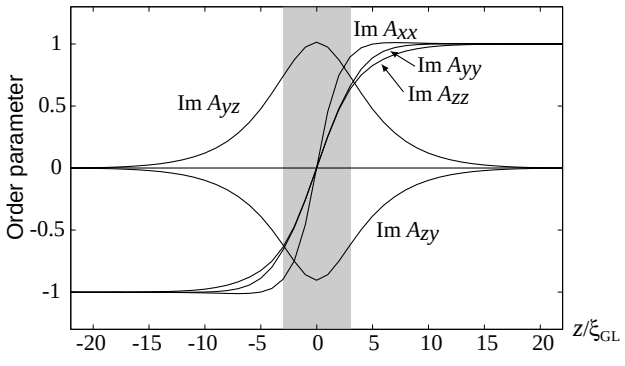

FIG. 3. The order parameter in the π state along the axis z of the aperture. The figure corresponds to the phase difference $\phi = \pi$, i.e., the order parameters far left and far right differ by factor -1. The broken symmetry allows nonzero A_{yz} and A_{zy} which have a long tail in the bulk. These components vanish in the zero branch. The wall is shown as shaded, $W = 6\xi_{GL}$ and $D = 10\xi_{GL}$.

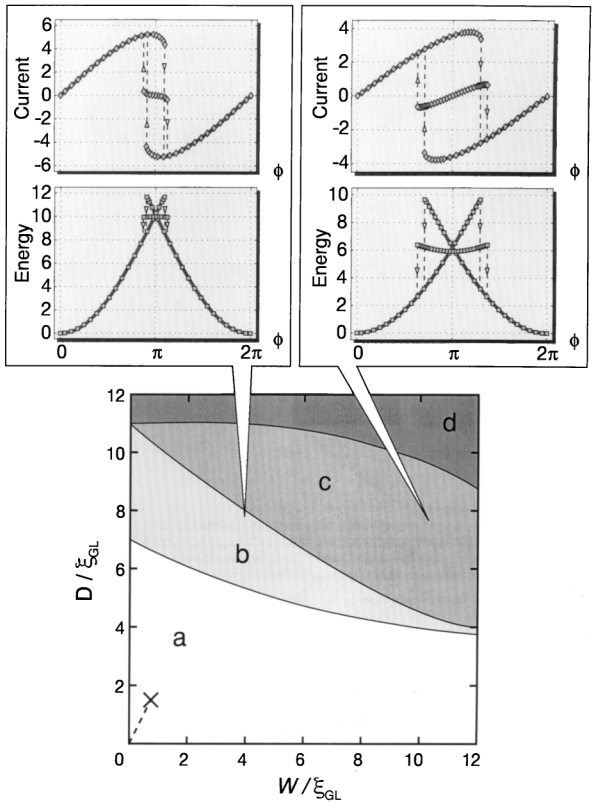

FIG. 4. Theoretical phase diagram for the π state in a single aperture. The current and the energy as a function of phase difference ϕ are shown in two cases. D is the diameter of the aperture and W is the wall thickness. The π branch is found in regions (*b*)–(*d*), where it is locally stable at a fixed phase difference $\phi \approx \pi$. In regions (*c*) and (*d*) it is also a local minimum of energy with respect to ϕ at $\phi = \pi$. In regions (*b*) and (*c*) the π state is the absolute minimum energy state at $\phi = \pi$. The parameters of *one* aperture of the experimental aperture array [2] are shown by the dashed line, and the observation of the π state is marked by a cross. The temperature dependent GL coherence length is defined by $\xi_{GL} = \hbar v_F/\sqrt{10}\,\Delta(T)$, where v_F is the Fermi velocity and $\Delta(T)$ is the Bardeen-Cooper-Schrieffer energy gap.

single aperture. The reason is that whenever it is locally stable, there always exists a locally stable zero state at the same ϕ. Because the order parameters of the π and zero states differ considerably, it may be that the phase slips take place only between two branches of the zero state without ever finding the way to the lower energy π state. This is what we find in the numerical calculations, where the π state was found only if the initial $A_{\mu j}$ was chosen close enough to the converged solution. We recall, though, that our calculations are not meant to simulate the correct dynamics of the phase slip.

The dimensions of one aperture in the array at Berkeley are marked in Fig. 4. This is clearly in the region where no π state is found. Although the Ginzburg-Landau calculation is accurate only at temperatures near T_c, it is unlikely that the π state could be stabilized in a more accurate calculation at lower temperatures. This statement is based on experience gained in previous low-temperature calculations [18]. Thus we conclude that the appearance of the π state in the Berkeley experiment essentially depends on the presence of many apertures.

We have also done two-dimensional calculations that simulate the flow through a long narrow slit. The π state is found and its properties are qualitatively similar to those in a circular aperture [19]. In particular, the transitions from the zero branch to the π branch seem to be absent. This is consistent with the fact that no π branch was found in the experiments by Avenel and Varoquaux [1].

The π state can be interpreted so that a *half-quantum* vortex has crossed the orifice. There are no free half-quantum vortices in superfluid ^{3}He-B, but the double-core vortex [20] can be interpreted as a bound pair of two half-quantum vortices [21]. Indeed, the order parameter in Fig. 3 is very similar to that in the double-core vortex on the axis going between the two cores [20].

Conclusion.—The π state was found to occur in both the limits investigated above. Its mechanism is the same in both cases: a lower coupling energy is achieved by producing a spin-orbit rotation that heals slowly in the bulk liquid. The Berkeley experiment [2] is somewhat an intermediate case to the two limits studied, which makes it evident that the π state there also arises from the same mechanism.

The theory above provides several predictions which can be tested experimentally. For example, the π state depends on the linear dimension L of the aperture array because α/γ, $\beta/\gamma \propto L$. An external magnetic field fixes the surface orientation of $\hat{\mathbf{n}}$, and thus can be used to suppress the π state.

Note added.—Quite recently, the π state has been experimentally observed also in a single narrow slit [22].

[1] O. Avenel and E. Varoquaux, Jpn. J. Appl. Phys. **26**, Suppl. 3, 1798 (1987); Phys. Rev. Lett. **60**, 416 (1988).

[2] S. Backhaus, S. Pereverzev, R. W. Simmonds, A. Loshak, J. C. Davis, and R. E. Packard, Nature (London) **392**, 687 (1998).

[3] A. Marchenkov, R. W. Simmonds, S. Backhaus, A. Loshak, J. C. Davis, and R. E. Packard, Phys. Rev. Lett. **83**, 3860 (1999).

[4] N. Hatakenaka, Phys. Rev. Lett. **81**, 3753 (1998); J. Phys. Soc. Jpn. **67**, 3672 (1998).

[5] O. Avenel, Y. Mukharsky, and E. Varoquaux, Nature (London) **397**, 484 (1999).

[6] L. N. Bulaevskii, V. V. Kuzii, and A. A. Sobyanin, JETP Lett. **25**, 290 (1977).

[7] S. Yip, Phys. Rev. B **52**, 3087 (1995).

[8] V. Ambegaokar, P. G. deGennes, and D. Rainer, Phys. Rev. A **9**, 2676 (1974); **12**, 345 (1975).

[9] See, for example, M. Tinkham, *Introduction to Superconductivity* (McGraw-Hill, New York, 1996), 2nd ed.

[10] A. J. Leggett, Ann. Phys. (N.Y.) **85**, 11 (1974).

[11] W. F. Brinkman, H. Smith, D. D. Osheroff, and E. I. Blount, Phys. Rev. Lett **33**, 624 (1974).

[12] E. V. Thuneberg, Europhys. Lett. **7**, 441 (1988).

[13] Note that this procedure limits the grazing-angle quasiparticles more than the cosine law usually employed in pinhole calculations [14].

[14] J. Kurkijärvi, Phys. Rev. B **38**, 11 184 (1988).

[15] W. Zhang, J. Kurkijärvi, and E. V. Thuneberg, Phys. Rev. B **36**, 1987 (1987).

[16] M. C. Cross, J. Low Temp. Phys. **21**, 525 (1975).

[17] S. Ullah and A. L. Fetter, Phys. Rev. B **39**, 4186 (1989).

[18] E. V. Thuneberg, J. Kurkijärvi, and J. A. Sauls, Physica (Amsterdam) **165B–166B**, 755 (1990).

[19] The earlier calculation [12] missed the π state (in the case of parallel $\hat{\mathbf{n}}$'s) probably because the area of calculation around the orifice was chosen too small.

[20] E. V. Thuneberg, Phys. Rev. B **36**, 3583 (1987).

[21] G. E. Volovik, Pisma Zh. Eksp. Teor. Fiz. **52**, 972 (1990) [JETP Lett. **52**, 358 (1990)].

[22] O. Avenel, Yu. Mukharsky, and E. Varoquaux, Physica B (to be published).